CHARACTERIZATION OF NH$_3$ SENSING PROPERTIES OF P3HT+RGO+CNT COMPOSITE FILMS MADE BY SPIN-COATING

LAM MINH LONG[1], NGUYEN NANG DINH[1,†], AND TRAN QUANG TRUNG[2]

[1]*University of Engineering and Technology,*
VNU in Hanoi, No. 144 Xuan Thuy Road, Cau Giay District, Hanoi, Vietnam

[2]*University of Natural Science, VNU in Ho Chi Minh City,*
227 Nguyen Van Cu Road, District 5, Ho Chi Minh City, Vietnam

[†]*E-mail:* dinhnn@vnu.edu.vn

Abstract. *Thin films of poly(3-hexylthiophene) (P3HT) incorporated with reduced graphene oxide (rGO) and multi-walled carbon nanotubes (CNTs) were prepared by spin-coating technique. Atomic force microscope (AFM) surface morphology, UV-Vis spectra and NH$_3$ gas sensing of the films were studied. Results showed that the P3HT embedded with a content of 20 wt.% of rGO and 10 % of CNTs (abbreviated to P3GC) resulted in the formation of nanostructured composites, exhibiting 1.50 nm-roughness surface and a semiconducting material with a bandgap of 1.92eV. These structure and composition of the P3GC film are appropriate for making film sensors, whose resistance changes as a function of gas concentration. Monitoring ammonia gas by the sensors showed that the responding time of the sensing reached a value as fast as 30 s, the response at ammonia gas content of 10 ppm attained a value as large as 0.8% and the relative sensitivity was of 0.05 %/ppm.*

Keywords: P3HT+rGO+CNT composite; surface morphology; UV-Vis spectra; NH$_3$ gas sensors; sensing response.

Classification numbers: 78.30.C-; 73.50.-h; 74.25.nd; 07.07.Df.

I. INTRODUCTION

Ammonia is a compound of nitrogen and hydrogen with the formula NH$_3$. It contributes significantly to the nutritional needs of terrestrial organisms by serving as a precursor to food and fertilizer. With the development of the chemical industry, more and more generation of ammonia gas is brought into the environment. It is known that ammonia gas is a toxic compound, consequently it is harmful to human health when a large enough concentration of this compound is attained [1]. Thus production of devices (or sensors) to detect ammonia gas with a large sensitivity and selective property is very important. Many scientific groups have researched and developed gas ammonia sensors for applications. Sensors based on nanostructured inorganic structures like SnO$_2$, WO$_3$, TiO$_2$, etc. have large sensitivity and response time, but the technology for producing both the materials and devices for gas sensors usually requests vacuum and high temperature that results in considerably large expenses [2]. With the aim to reduce these costs, many scientific groups have developed gas sensors based on conducting polymers [3–5]. The advantage of the polymers based sensors consists of easy fabrication, low power consumption, room temperature operation, etc. [6]. Among the conducting polymers, polyethylenedioxythiophene + poly(4-styrenesulfonate) (PEDOT:PSS) is the most utilized in organic light emitting diode (OLED) and in organic solar cells (OSCs). PEDOT:PSS is also used for producing gas like CO [7], NH$_3$ [8] and vapors of organic solvents or water [9, 10]. We recently reported that PEDOT:PSS based sensors can detect both ammonia gas [11] and humidity [12]. We have in particular observed that PEDOT:PSS+rGO+AgNWs based sensors are sensitive to relative humidity (RH%) at a value as low as 30% [12]. This ability for detecting humidity is however a disadvantage when monitoring ammonia or other gases in a humid environment is considered. For practical applications we need a sensor that is not only sensitive to the gas to be measured, but also selectively detecting towards the gas.

During our study of OSCs using poly(3-hexylthiophene) (P3HT) as a photoactive layer [13], we recognized that P3HT films synthetized in air with a humidity larger than RH%60 exhibited a quality as good as when it was synthetized in a dried nitrogen glove-box. This would show that the P3HT structure was not affected by the absorption of water vapor. This observation prompted us to investigate the preparation and characterization of potential P3HT+rGO+CNT sensors for detecting ammonia gas. The present work is thus focused on the preparation of P3HT+rGO+CNT composite films and sensing devices for measurements of ammonia gas in a concentration range from 10 to 50 ppm.

II. EXPERIMENT

II.1. Preparation of rGO solution

All chemicals like P3HT and multiple wall CNTs, with purity of $\geq$ 99.9% were purchased from Sigma-Aldrich Corporation. To prepare reduced graphene oxide (rGO), graphite flakes (GF) were taken off from graphite pieces with fewer layers by microwave heating solution of graphite filled in KMnO$_4$ and HNO$_3$. Mixtures of 0.2 g GF, 0.2 g NaNO$_3$ and 9.6 ml H$_2$SO$_4$ were put in a 200 mL volume Corning-247 glass beaker, then 1.2g KMnO$_4$ and 28 ml of distilled water was poured into the glass beaker to get a liquid solution. Next, 10 ml H$_2$O$_2$ was added to this solution and ultrasonically stirred at room temperature for 8 hours to separate MnO$_4^-$ and MnO$_2$ into Mn$^+$ ions, yielding a solution with a bright-yellow color. The obtained solution was unmoved for 24

hours, and at the glass beaker bottom a paste-like layer with dark-yellow color was deposited, constituting the rGO paste. By slowly sucking, the solution above the rGO paste was completely taken from the glass beaker. Finally, 0.2 g of rGO paste was diluted in 40 ml of N,N-dimethylformamide (DMF) solvent in 50 ml-volume glass beaker and ultrasonically stirred for 900s to get completely dispersive rGO in DMF (rGO-DMF). After 24 hours waiting for the solution stabilization, 30 ml of rGO-DMF solution from the glass beaker top was taken and kept in another glass beaker for further use.

II.2. Preparation of P3HT+rGO+CNT composite solution

P3HT powder with a volume of 6 mg was mixed in 0.6 ml of rGO-DMF solution. This solution was ultrasonically stirred for 2 hours at room temperature. At the same time, 1 mg of multi-walled carbon nanotubes (shortly called CNTs) was embedded in 0.5 ml of DMF (CNT-DMF) and also stirred by ultrasonic machine for 1 hour. Finally, mixtures of the rGO-DMF and CNT-DMF solutions were put in a small glass beaker and carefully stirred for 5 hours at 80°C by using a magnetic stirrer. For all the volumes of chemicals of P3HT, rGO and CNTs used for further solid film preparation, the weight ratio of P3HT:rGO:CNTs was 100:20:10 (namely, the volume content of rGO and CNTs embedded in P3HT matrix was chosen to be respectively 20 wt.% and 10 wt.%. For simplicity in further analysis, the composite samples with such contents of P3HT, rGO and CNTs were abbreviated to P3GC.

Using spin-coating, P3GC solutions were deposited onto glass substrates which were coated by two silver planar electrode arrays with a length of 4 mm and separated from each other by a distance of 2 mm. The following parameters were used for spin-coating: a delay time of 100 s, a rest time of 45s, a spin speed of 1500 – 1800 rpm, an acceleration of 500 rpm, and finally a drying time of 300s. To dry the composite films, a flow of dried gaseous nitrogen was used for 10 hours. For a solidification avoiding the use of solvents, the film samples were annealed at 120°C for 2 hours in a "SPT-200" vacuum drier.

II.3. Characterization techniques

The surface morphology of samples was characterized by using a "Hitachi S-4800" field emission scanning electron microscopy (FE-SEM). Atomic force microscope (AFM) images were obtained using a NT-MDT atomic force microscope operating in a tunnel current mode. Crystalline structures were investigated by X-Ray diffraction (XRD) with a Philips D-5005 diffractometer using filtered CuKα radiation ($\lambda = 0.15406$ nm). The ultraviolet-visible absorption spectra were carried out on a Jasco UV-Vis-NIR V570.

For monitoring gases, the prepared sensing samples were put in a testing chamber of 10 dm^3 in volume. The gases value can be fixed in a rage from 10 to 1000 ppm by use of an "EPA-2TH" profilometer (USA). To characterize the gas sensitivity of the samples, the devices were placed in a test chamber at the room temperature (namely 300 K) and the Ar gas pressure of 101.325 kPa (or 1 Atm); the device electrodes were connected to electrical feedthroughs. The measurements that were carried-out included two processes: adsorption and desorption. In the adsorption process, the gas (or vapor) flow consisting of Ar carrier and measuring vapor from a bubbler was introduced into the test chamber for an interval of time, following which the change in resistance of the sensors was recorded. In the desorption process, a dried Ar gas flow was inserted in the chamber in order to recover the initial resistance of the sensors. Through the recovering time dependence of

the resistance one can obtain information on the desorption ability of the sensor in the desorption process.

The P3GC film sensors were exposed to NH$_3$ gas with concentration (C_{gas}) that was controlled with step decreases from 50 ppm to 40, 30, 20 and 10 ppm. The repeatability in the resistance change of P3GC sensor was studied by measuring the resistance of sensor as a function of both the insertion/extraction of ammonia gas in/out chamber and measurement time. Each measurement cycle consists of the following time durations: 20 seconds for NH$_3$ gas detecting to saturation state, 50 seconds for maintaining exposed ammonia gas in chamber with above-mentioned concentrations (namely C_{gas} = 50, 40, 30, 20 and 10 ppm), 30 seconds for extraction of Ar and ammonia gas out from chamber; then 20 seconds for heating samples at 70˚C for completing extraction of NH$_3$ and finishing the prior cycle. The next cycle was repeated by the same steps.

III. RESULTS AND DISCUSSION

III.1. Morphology and crystalline structure of P3HT-based films

Figure 1 shows AFM images of a pure P3HT and an anealled P3GC composite films. The thickness of the film is 550 nm, the annealing temperature is 120˚C and the annealing time is 2 hours. This figure shows that the pure P3HT film exhibited a smooth surface (Fig. 1a), whereas the roughness of the P3GC film surface was estimated as about 1.50 nm (Fig. 1b). Thus the roughness of the P3GC film can be attributed to the presence of both rGO and CNTs nano particles. The roughness and porosity of the composite sample were also observed by FE-SEM micrograph (Fig. 2) where P3HT polymer matrix is not revealed in the FE-SEM. This figure clearly shows the presence of the multi-walled carbon nanotubes in the P3GC sample.
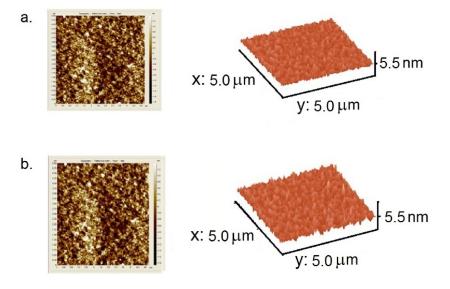

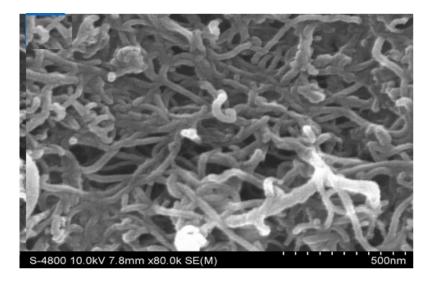**Fig. 1.** AFMs of a pure P3HT (a) and P3GC (b) film annealed at 120˚C for 2 hours.

Fig. 2. FE-SEM of a P3GC composite film.

A XRD pattern of a P3GC film is shown in Fig. 3. In a 2θ range from 2 to 30 degrees two characteristic peaks are observed: the $2\theta = 5.5^o$ peak is consistent with the peak for P3HT [14] and the 26.1^o peak belongs to rGO as reported in [15]. There are no peaks reflecting the presence of the CNTs, because the structure of CNTs exhibit nanotubes, but not crystalline lattice, consequently no X-ray diffraction appeared.
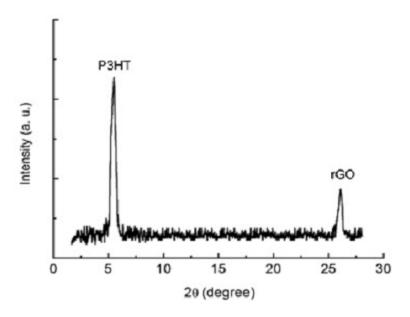

Fig. 3. XRD patterns of a P3GC film. Thickness is $d = 550$ nm.

Full width at half maximum (FWHM) of P3HT and rGO peaks is rather large. This shows that both the P3HT and rGO were formed in nanocrystalline particles. Using Scherrer formula, the calculated particles size (τ) can be found:

$$\tau = \frac{0.9 \times \lambda}{\beta \times cos\theta} \qquad (1)$$

where λ is the wavelength of the X-ray used for incident radiation. In our experiment Cu-tube was used, thus $\lambda = 0.15406$ nm, β the FWHM (in radians) and θ is the diffraction angle of the considered peak [16].

From the XRD pattern in Fig. 3 for the P3HT peak, $\beta = 0.0044$, τ was found to be of ca. 30 nm. For the rGO peak, $\beta = 0.0034$, consequently $\tau \approx 40$ nm. The nanoparticles of P3HT and rGO combining with the CNTs in the P3HT+rGO+CNT composite have created numerous nano-heterojunctions of P3HT/rGO, P3HT/CNT. Since both the content of rGO and CNTs embedded in the polymer is small, only a few random heterojunctions of rGO/CNT could be formed. Herein the CNTs play the role of bridges connecting together rGO and P3HT particles, due to which the charge carriers could move more easily from one particle to another, when an electrical field is applied onto the films.

III.2. Ammonia gas sensing of P3HT-based films

The results for the measurements of 5 cycles according to the ammonia concentration from 50, 40, 30, 20 and 10 ppm are shown in Fig. 4. The cyclic behavior of the sensor performance shows that the P3GC sensors exhibited a good reversible sensing property torward ammonia gas. With exposition of ammonia gas in chamber, the sensor resistance increased rapidly, reaching the saturation value in about 20 seconds; and recovering its initial value in about 30 seconds after the extraction of ammonia gas from the chamber.
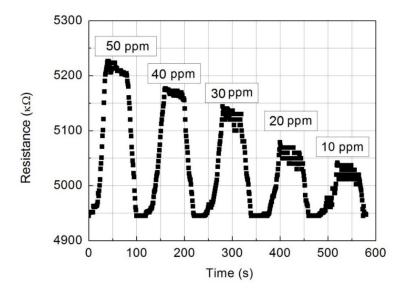

Fig. 4. Time dependence of resistance of P3GC film on repeated exposure and removal of NH₃ gas.

The increase in resistance of the P3GC sensor is closely related to a lowering of major charge carriers (namely holes) in P3HT polymer that is considered as a p-type organic semiconductor [17]. Whereas NH_3 is a highly active and electron donating free radical [4], electrons generated by the absorption of ammonia gas on the surface of P3GC film eliminated a part of holes by coupling with each other, resulting in an increase of the P3HT resistance. When the P3GC film was slightly heated, NH_3 molecules in P3HT rapidly evaporated from the film surface, leaving holes along the backbone of the polymer. In such fashion, the concentration of major charge carriers rapidly increases while the resistance of the sensor decreases.

Embedding rGO in P3HT have enabled to enhance sensing properties of the P3GC films. This is similar to the results reported in [18] for polypyrrole (Py)-rGO-based sensors, where the authors explained the excellent sensing properties of Py-rGO based sensors due to the parts of oxygen-based moieties and structure defects after chemical reduction process, resulting to the p-type semiconducting behavior of the resultant rGO. NH_3, as a reducing agent, has a lone electron pair that can be easily donated to the p-type rGO sheets, leading to the increase of the resistance of the rGO devices. Whereas multi-walled CNTs have contributed to improve the adsorption efficiency of gas-molecules (included NH_3) due to larger effective surface areas with many sites, as suggested by Varghese *et al.* [19]. Moreover, the addition of rGO and CNTs together in P3GC composite films created not only numerous nano-heterojunctions of P3HT/rGO and P3HT/CNT, but also nanotube "bridges" for electrons transferring. These "bridges" are clearly revealed by the SEM micrograph, as shown in Fig. 2. In [13] we also demonstrated that inorganic nanoparticles embedded in polymers filled-up most of the cracked spots in polymers that were often created during post-annealing. By this way, the cracked spots served as charge traps were eliminated in nanocomposite films. With the presence of nano-heterojunctions of P3HT/rGO and P3HT/CNT that together reduced the charge traps, one can enhance the performance of the sensors made from P3GC films.

To characterize better the sensing performance of sensors, the sensing response (η) of the device has been used. It is determined by following equation:

$$\eta = \frac{R - R_0}{R_0} (\%) \tag{2}$$

where R_0 is the initial resistance of the sensor, namely 4945 kΩ in our experiments. Results of the η calculation were plotted in Fig. 5, showing the η-C_{gas} dependence.

The responding time of the sensor was about 30s and the resistance of the P3GC composite films fast recovered to baseline when exposed to air. In the same period of time (namely 30 s), the sensing response to NH_3 with C_{gas} lowering from 50 to 40, 30, 20 and 10 ppm decreased from 2.9 to 2.4, 1.8, 1.3 and 0.8%, respectively. Figures 4 and 5 show that the detection limit for NH_3 gas can be attained a value lower than 10 ppm. However, using the EPA-2TH gas profilometer, we could not introduce NH_3 gas with an accurate concentration in the range from 0 to 10 ppm.

From Fig. 5 one can see that the response of the sensor linearly decreases with decreases in ammonia gas concentration; and the slope of the linear plot reflects the relative sensitivity of the sensor. Thus, for the P3GC composite film sensor, the relative sensitivity was found to be of 0.05 %/ppm. This value is about two times larger than the sensitivity of the ammonia gas sensor made from PEDOT:PSS [20].
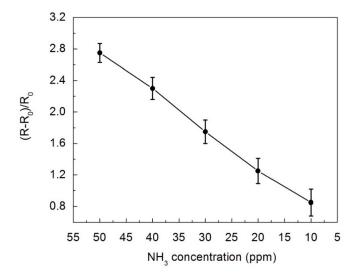
Fig. 5. Sensitivity of P3GC sensor vs. ammonia concentration.

IV. CONCLUSION

Using spin-coating technique, films of P3HT embedded with rGO nanoparticles and CNTs were prepared. The AFM surface morphology, XRD structural analysis and UV-Vis spectra of the films were done. Ammonia gas sensing was performed thanks to measurements of the film resistance as a function of time and gas concentration during NH_3 adsorption/desorption processes. The results obtained showed that the P3HT embedded with a content of 20 wt.% of rGO and 10% of CNTs resulted in the formation of nanostructured composites called P3GC that caused effective absorption/desorption of ammonia gas on/out of the film surface. P3GC based sensors possessed a responding time of ca. 30 seconds, a sensing response of 0.8% at ammonia gas concentration of 10 ppm and a relative sensitivity of 0.05%/ppm.

REFERENCES

[1] T. Hibbard, K. Crowley, and A. J. Killard, *Analytica Chimica Acta*, **779** (2013) 6.

[2] M. Gardon and J. M. Guilemany, *Journal of Materials Science* **24** (2013) 1410.

[3] J. Janata and M. Josowicz, *Nature Materials* **2** (2003) 19.

[4] H. Bai and G. Shi, *Sensors*, **7** (2007) 267.

[5] T. Patois, J.-B. Sanchez, and F. Bergeretal, *Talanta* **17** (2013) 45.

[6] Y.-S. Lee, B.-S. Joo, N.-J. Choi, J.-O. Lim, J.-S. Huh, and D.-D. Lee, *Sensors and Actuators B* **93** (2003) 148.

[7] S. Basu and P. Bhattacharyya, *Sensors and Actuators B* **173** (2012) 1.

[8] P. T. Yin, T. H. Kim, J. W. Choi, and K. B. Lee, *Physical Chemistry Chemical Physics* **15** (2013) 12785

[9] B. H. Chu, J. Nicolosi, C. F. Lo, W. Strupinski, S. J. Pearton, and F. Ren, *Electrochemical and Solid State Letters* **14** (2011) K43.

[10] M. Zhang and Z. Wang, *Applied Physics Letters* 102 (2013) 213104.

[11] Lam Minh Long, Nguyen Nang Dinh, Hoang Thi Thu, Huynh Tri Phong, and Tran Quang Trung, *VNU Journal of Science.: Mathematics – Physics*, **33** (2017) 52.

[12] Lam Minh Long, Nguyen Nang Dinh, Tran Quang Trung, *Journal of Nanomaterials* **2016** (2016) 5849018.

[13] Tran Thi Thao, Tran Quang Trung, Vo-Van Truong, Nguyen Nang Dinh, *Journal of Nanomaterials* **2015** (2015) 463565.

[14] N. Abu-Zahra and M. Algazzar, *Journal of Solar Energy Engineering* **136/2** (2013) 021023.

[15] L. Stobinski, B. Lesiaka, A. Malolepszyc, M. Mazurkiewiczc and B. Mierzwaa, *Journal of Electron Spectroscopy and Related Phenomena* **195** (2014) 145.

[16] B. D. Cullity, *Elements of X-Ray diffraction*, 2nd ed., p. 102, Addison-Wesley Publishing Company, Inc., Reading, MA, 1978.

[17] B. M. Omer, *Journal of Nano and Electronic Physics* **5** (2013) 03010.

[18] Y. Wang, L. Zhang, N. Hu, Ying Wang, Y. Zhang, Z. Zhou, Y. Liu, S. Shen, and C. Peng, *Nanoscale Research Letters* **9** (2014) 251.

[19] O. K. Varghese, P. D. Kichambre, D. Gong, K. G. Ong, E. C. Dickey, and C. A. Grimes, Sensors and Actuators B 81 (2001) 32.

[20] L. Aba, Y. Yusuf, Mitrayana, and K. Triyana, *Journal of Modern Physics*, **3** (2012) 529.